ORGANOMETALLICS

Article

pubs.acs.org/Organometallics

From Sunscreen to Anticancer Agent: Ruthenium(II) Arene Avobenzone Complexes Display Potent Anticancer Activity

Riccardo Pettinari,*[,†] Fabio Marchetti,[‡] Agnese Petrini,[†] Claudio Pettinari,[†] Giulio Lupidi,[†] Piotr Smoleński,[§] Rosario Scopelliti,[∥] Tina Riedel,[∥] and Paul J. Dyson*[,∥]

[†]School of Pharmacy and [‡]School of Science and Technology, University of Camerino, via S. Agostino 1, 62032 Camerino, Macerata, Italy

[§]Faculty of Chemistry, University of Wrocław, ul. F. Joliot-Curie 14, 50-383 Wrocław, Poland

[∥]Institut des Sciences et Ingénierie Chimiques, Ecole Polytechnique Fédérale de Lausanne (EPFL), 1015 Lausanne, Switzerland

Supporting Information

ABSTRACT: A series of ruthenium(II) arene derivatives (arene = cymene (cym), hexamethylbenzene (hmb)) containing avobenzone (1-(4-*tert*-butylphenyl)-3-(4-methoxyphenyl)propane-1,3-dione, AVBH) and PTA (1,3,5-triaza-7-phosphaadamantane) or PTA-Me (*N*-methyl-1,3,5-triaza-7-phosphaadamantane cation) have been synthesized and fully characterized. Three types of complexes have been obtained: i.e., neutral [Ru(arene)(AVB)Cl] (**1**, arene = cym; **2**, arene = hmb), monocationic [Ru(arene)(AVB)(PTA)][SO_3CF_3] (**3**, arene = cym; **4**, arene = hmb), and dicationic [Ru(arene)(AVB)(PTA-Me)][SO_3CF_3][BF_4] (**5**, arene = cym; **6**, arene = hmb). The solid-state structures of **1** and **2** were determined by single-crystal X-ray diffraction. The cytotoxicity of the complexes has been evaluated *in vitro* against human ovarian carcinoma cells, A2780 and A2780cisR, as well as against nontumorous Human Embryonic Kidney (HEK293) cells. The ionic complexes with hydrophilic PTA and PTA-Me ligands in **3**−**6** are considerably more active than the neutral complexes **1** and **2**.

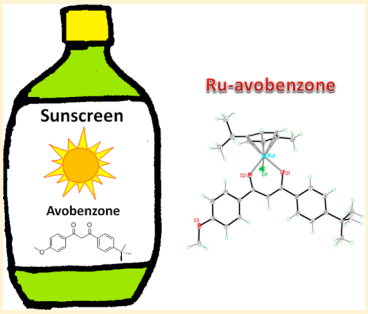

INTRODUCTION

In recent years, ruthenium complexes have emerged as promising antitumor agents with potential uses in platinum-resistant tumors and solid metastasis.[1−15] The two best known examples are indazolium *trans*-[tetrachloridobis(1*H*-indazole)-ruthenate(III)] (KP1019)[10,11,16] and imidazolium *trans*-[tetrachlorido(*S*-dimethyl sulfoxide)(1*H*-imidazole)ruthenate-(III)] (NAMI-A),[17−20] since both have been evaluated in clinical trials. A prominent example of an organometallic ruthenium-based compound is [Ru(cymene)Cl_2(PTA)], termed RAPTA-C (PTA = 1,3,5-triaza-7-phosphaadamantane),[21] which exhibits generally low cytotoxicity *in vitro*[22,23] but relevant antimetastatic[24,25] and antiangiogenic[26,27] properties *in vivo*. Moreover, it has recently been shown that RAPTA-C reduces the growth of primary tumors in preclinical models for ovarian and colorectal carcinomas via an antiangiogenic mechanism.[28] In addition to a large number of RAPTA-based derivatives,[29] a wide and diverse range of other ruthenium(II) arene complexes with N,N-, N,O-, and O,O-chelating ligands have shown promising therapeutic potential.[30−36]

A key strategy has been to employ chelating ligands that exhibit known bioactive properties.[37−40] In this respect, here we investigate the ligating potentials of avobenzone (1-(4-*tert*-butylphenyl)-3-(4-methoxyphenyl)propane-1,3-dione, AVBH), a common oil-soluble UVA filter employed extensively in the formulation of sunscreens and cosmetic products.[41] AVBH absorbs UV rays and converts them into heat that is dispersed in the skin. More recently, however, AVBH has been shown to exhibit promising anticancer properties, especially against a chemoresistant cancer cell type, where it showed efficacy similar to that of doxorubicin.[42] Doxorubicin is a known DNA intercalator disrupting topoisomerase II mediated DNA repair.[43] In addition, it generates free radicals and causes damage to cellular membranes, DNA, and proteins, a mechanism interesting to explore for the action of AVBH in cancer cells, as it can induce similar effects. Motivated by the activity of AVBH against cancer cells, we designed ruthenium(II) AVBH complexes with the focus on enhancing the overall hydrophilicity to ensure increased cellular uptake of AVBH and at the same time tuning their activity by introducing PTA or PTA-Me as a coligand.

RESULTS AND DISCUSSION

Complexes **1** and **2** were prepared in high yield from the reaction of the appropriate dimer [Ru(arene)Cl_2]$_2$ (arene = cymene, hexamethylbenzene) with AVBH and KOH in methanol (Scheme 1). The complexes are air-stable and are soluble in alcohols, acetone, acetonitrile, chlorinated solvents, DMF, and DMSO and sparingly soluble in diethyl ether. The IR spectra of **1** and **2** show the typical shift of the ν(C═O) vibrations to lower wavenumber upon coordination of the

Received: August 31, 2016

DOI: 10.1021/acs.organomet.6b00694
Organometallics XXXX, XXX, XXX−XXX

Scheme 1. Synthesis of 1 and 2

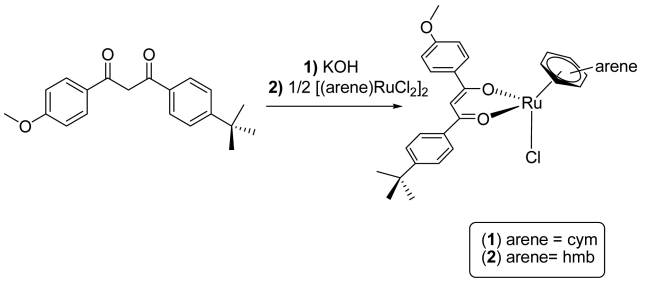

AVBH proligand to the ruthenium ion.[44] In the far-IR region, absorptions were observed at 274 and 279 cm^{-1} which correspond to ν(Ru−Cl) stretches.[45] The electrospray ionization (ESI) mass spectra of **1** and **2** display peaks corresponding to the appropriate $[Ru(arene)(AVB)]^+$ ion: i.e., generated via dissociation of the chloride ligand. The ^1H and ^{13}C NMR spectra of **1** and **2** recorded in $CDCl_3$ corroborate the expected structures containing the bidentate AVB ligand. Conductivity measurements indicate a slight dissociation of the chloride in CH_3CN at room temperature.

The chloride ligand in **1** and **2** is readily replaced by the amphiphilic, cagelike aminophosphine 1,3,5-triaza-7-phosphaadamantane (PTA), by treatment with $AgSO_3CF_3$ in methanol containing PTA, affording $[Ru(cym)(AVB)(PTA)][SO_3CF_3]$ (**3**) and $[Ru(hmb)(AVB)(PTA)][SO_3CF_3]$ (**4**), as depicted in Scheme 2.

Scheme 2. Synthesis of 3 and 4

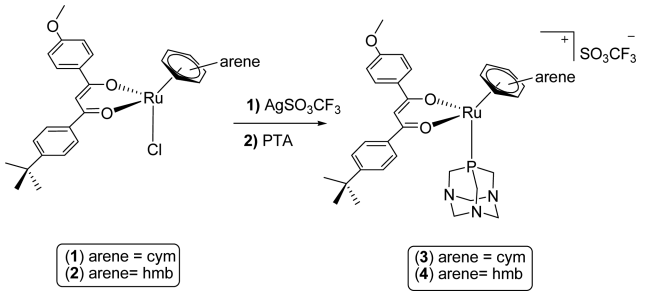

The substitution of the chloride ligand by PTA and the formation of the ionic compounds were confirmed by the disappearance of the ν(M−Cl) band in the IR spectra of **3** and **4**. Moreover, a characteristic absorption pattern in the region 1000−1200 cm^{-1}, indicative of a noncoordinated $O_3SCF_3^-$ anion, is observed.[46] The ^1H NMR spectra of **3** and **4** in CD_3CN display the expected signals due to the coordinated arene, AVB, and PTA ligands. The ^{31}P NMR resonances due to PTA are observed at lower field with respect to those of uncoordinated PTA, thus confirming coordination to the metal center.[47] The conductance values in acetonitrile confirm the existence of 1:1 electrolyte species for **3** and **4**.[48]

Similarly, **1** and **2** can be transformed by reaction with the *N*-methyl-1,3,5-triaza-7-phosphaadamantane cation (PTA-Me), in the presence of $AgSO_3CF_3$, into the dicationic species $[Ru(cym)(AVB)(PTA\text{-}Me)][SO_3CF_3][BF_4]$ (**5**) and $[Ru(hmb)(AVB)(PTA)][SO_3CF_3][BF_4]$ (**6**) (see Scheme 3).

For **5** and **6** the formation of dicationic species, with characteristic absorption patterns in the region 1000−1200 cm^{-1} which are indicative of noncoordinated $O_3SCF_3^-$ and BF_4^- anions, are observed.[46] The conductance values of **5** and **6**

Scheme 3. Synthesis of 5 and 6

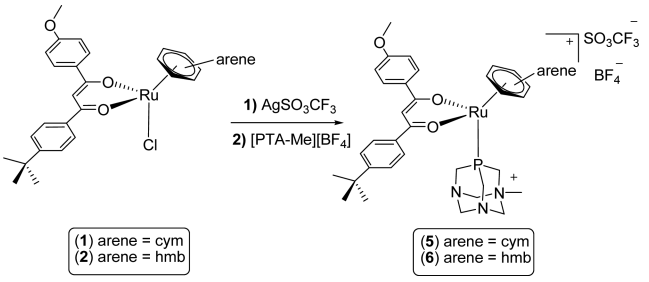

in an acetonitrile solution further confirm the existence of 2:1 electrolyte species.[48] The stability of all the complexes in DMSO was investigated. Solutions of the complexes (c = 20.0 mM) in DMSO were prepared, and their stability was monitored for 72 h by ^1H and ^{31}P NMR spectroscopy. Complexes **1** and **2** immediately underwent ligand exchange by ca. 15%, which remained constant during the following 72 h. Complex **3** showed a small amount of ligand exchange (ca. 10%) after 72 h, whereas **5** immediately underwent a ligand exchange. The ligand exchange process probably involves breaking a Ru−O bond followed by exchange with a solvent molecule. Note that the ^{31} P NMR spectra of **3** and **5** display a unique resonance for coordinated PTA and remain unchanged within 96 h. In contrast, the hexamethylbenzene derivatives **4** and **6** were stable during the 72 h period (Figures S1−S6 in the Supporting Information). The stability of ionic complexes **3**−**6** was also determined under pseudopharmacological conditions in NaCl solution (5 mM, corresponding to the low intracellular NaCl concentration in cells) and in 100 mM NaCl solution (approximating to the higher chloride levels in blood). Solutions of the complexes (c = 2.0 mM) in aqueous NaCl (c = 5 or 100 mM in D_2O containing 10% of $[D_6]$DMSO) were prepared and maintained at 37 °C for 96 h and monitored by ^1H and ^{31}P NMR spectroscopy. None of the complexes were observed to change under either of the conditions: i.e., the ^1H and ^{31}P NMR spectra of **3**−**6** remained unchanged after 96 h (Figures S7−S10 in the Supporting Information). The molecular structures of **1** and **2** were confirmed by single-crystal X-ray structure analysis (see the Experimental Section and Supporting Information for details of the data collection and structure refinements). The molecular structures of **1** and **2** are shown in Figure 1, and relevant crystallographic parameters are reported in Table S1 in the Supporting Information.

Both complexes show a typical piano-stool geometry with central chirality at the metal ion and, despite having in some cases enantiomerically pure crystals, we made no attempt to separate and isolate the two enantiomers. From Figure 1 it is clear that the AVB ligand is O,O′-coordinated to the ruthenium ion, forming a six-membered metallacycle. The legs of the aforementioned piano-stool coordination around the metal center are completed by a Cl ligand and a cymene (Ru−centroid, 1.653(2) Å) in **1** or a hexamethylbenzene (Ru−centroid, 1.656(3) Å) in **2**. The AVB ligand displays, in both complexes, a twisted orientation with angles between the aromatic rings of 24.9° in **1** and 9.8, 24.1, and 15.2° in **2**. The values of the Ru−O_{av} and Ru−Cl distances are on average 2.067(3) and 2.435(1) Å in **1** and 2.086(5) and 2.428(2) Å in **2**, respectively.

Biological Studies. The cytotoxicities of **1**−**6** were evaluated in comparison to those of AVBH and cisplatin by determining the IC_{50} concentration against human ovarian

DOI: 10.1021/acs.organomet.6b00694
Organometallics XXXX, XXX, XXX−XXX

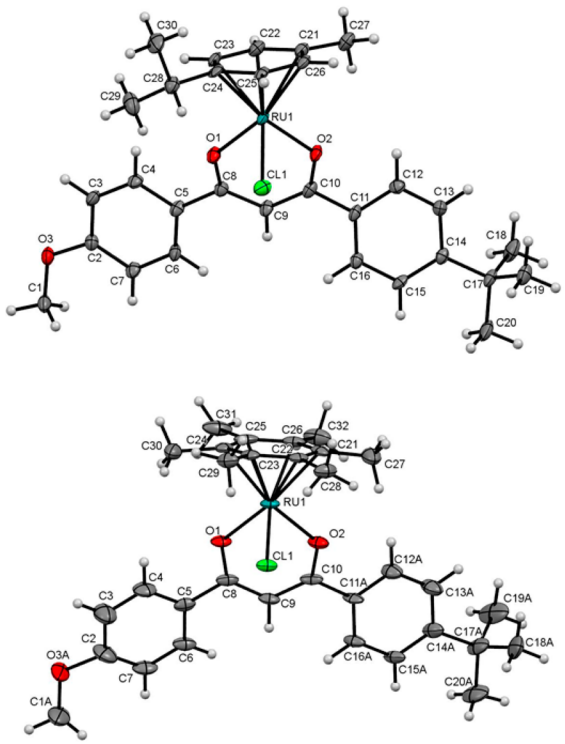

Figure 1. Ortep view of the molecular structures of **1** (top) and **2** (bottom). The probability threshold displayed for the ellipsoids is 50%. The asymmetric unit of **2** contains two independent molecules (only one is shown, for the sake of clarity). Selected bond distances (Å) and angles (deg) for **1**: Ru1−O1, 2.058(3); Ru1−O2, 2.076(3); Ru1−Cl1, 2.4348(13); O1−Ru1−O2, 88.13(12); O1−Ru1−Cl1, 84.30(9); O2−Ru1−Cl1, 85.00(9). Selected bond distances (Å) and angles (deg) for **2**: Ru1−O1, 2.088(4); Ru1−O2, 2.083(4); Ru1−Cl1, 2.4267(15); O1−Ru1−O2, 87.16(18); O1−Ru1−Cl1, 84.01(12); O2−Ru1−Cl1, 86.14(12).

carcinoma A2780 cells and the A2780cisR variant with acquired resistance to cisplatin, as well as against noncancerous human embryonic kidney (HEK293) cells. IC_{50} values for the compounds determined after 72 h of drug exposure are presented in Table 1.

In comparison to AVBH alone, which exhibits modest cytotoxicity but cancer cell selectivity, the mono- and dicationic complexes display a 10-fold increased potency in vitro against ovarian carcinoma (A2780 and A2780R) cell lines but do not display selectivity in comparison to the noncancerous cell type. The three types of complexes, neutral [Ru(arene)(AVB)Cl] (**1**, arene = cym; **2**, arene = hmb), monocationic [Ru(arene)(AVB)(PTA)]$^+$ (**3**, arene = cym; **4**, arene = hmb) and dicationic [Ru(arene)(AVB)(PTA-Me)]$^{2+}$ (**5**, arene = cym; arene = hmb, **6**), show the following trend of activity: monocationic > dicationic > neutral. Indeed, **4** is almost an order of magnitude more cytotoxic than cisplatin in the cisplatin-sensitive A2780 cell line (0.17 ± 0.01 vs 1.5 ± 0.4 μM).

Table 1. Cytotoxicities (IC_{50}, μM) of 1−6, AVBH, and Cisplatin following Incubation for 72 h with Non-Tumorous Human Embryonic Kidney HEK293 Cells and Human Ovarian Carcinoma A2780 and A2780R (Cisplatin-Resistant) Cell Lines

	IC_{50} (μM)		
compound	A2780	A2780cisR	HEK
1	17.7 ± 2.9	46.8 ± 4.1	32.5 ± 2.9
2	29.2 ± 4.8	48.1 ± 2.9	27.0 ± 1.5
3	0.41 ± 0.10	1.25 ± 0.11	0.74 ± 0.11
4	0.17 ± 0.01	1.57 ± 0.05	0.21 ± 0.09
5	0.70 ± 0.06	1.49 ± 0.07	1.47 ± 0.08
6	2.76 ± 0.24	3.74 ± 0.12	2.23 ± 0.10
AVBH	12.4 ± 1.1	15.6 ± 2.4	58.8 ± 4.6
cisplatin	1.4 ± 0.5	26.5 ± 2.3	11.2 ± 1.8

The DNA binding of AVBH and **1**−**6** was investigated by UV−visible spectroscopy,[49] and the absorption spectra were recorded in the presence of increasing amounts of calf thymus DNA (ct-DNA) (Figure S11 in the Supporting Information). The spectrum of avobenzone possesses a wide band near 370 nm, due to a $\pi-\pi^*$ transition of the enol form, with a shoulder near 380 nm and a weak band near 270 nm corresponding respectively to the n−π^* and $\pi-\pi^*$ transitions of the keto form.[50−52] Complexes **1**−**6** display intense absorptions due to the enol form of bonded avobenzone, shifted in the range 330−350 nm, together with a week band at 280−290 nm and a shoulder at 380 nm. Moreover, in the case of **1** and **2** a hypochromism is observed, accompanied by a small red shift of the band at 330−350 nm, whereas for **3**−**6** there is negligible hypochromism without any red shift. These results imply a relatively strong binding of neutral complexes **1** and **2** via intercalation, whereas the ionic complexes, **3**−**6**, likely interact with DNA through an electrostatic interaction.[53,54] The binding constants, K_b, of **1**−**6** with ct-DNA (Table 2), are on the order of 10^4 M^{-1}, with those of **1** and **2** being higher than those of **3**−**6**. However, such values are smaller than those of classical intercalators and metallo-intercalators, which are on the order of 10^7 M^{-1}.[55−57]

Competitive binding studies with ethidium bromide (EtBr) bound DNA were performed to further clarify the interactions of **1**−**6** with DNA. The emission spectra of the EB-ct-DNA system on addition of increasing amounts of **1**−**6** and AVBH are shown in Figure S12 in the Supporting Information. The emission band of the EB-ct-DNA system decreases in all cases, and the quenching parameters have been analyzed. The quenching constants K_{sv} and apparent DNA binding constants K_{app}, reported in Table 3, show that **1** and **2** are able to compete with EB-ct-DNA more efficiently than **3**−**6**.

In the presence of the DAPI intercalator specific for the DNA minor groove (DAPI, 4′,6-diamidino-2-phenylindole[58,59]), a pronounced decrease in the fluorescence intensity of the DAPI−ct-DNA complex was observed upon the addition of increasing concentrations of AVBH or complexes **1**−**6** (Figure S13 in the Supporting Information). The values of quenching constants K_{sv} (Table 2) again indicate that **1** and **2** display affinity higher than that of **3**−**6** for the minor groove of DNA.

Since the DNA binding studies do not correlate well with the observed cytotoxic effects of the compounds, protein binding studies were performed by tryptophan fluorescence quenching experiments using bovine serum albumin (BSA) as a model substrate in phosphate buffer at pH 7.4. Indeed, several recent studies reported that some cytotoxic Ru(II), Ru(III), Rh(III), and Ir(III) complexes were found to be able to interact with some plasma proteins[60−65] and with a number of cancer-related proteins, which may be responsible for the antiangiogenic and antimetastatic activity of Ru complexes.[66,67] The quenching of the emission intensity of tryptophan residues of BSA at 344 nm

DOI: 10.1021/acs.organomet.6b00694
Organometallics XXXX, XXX, XXX−XXX

Table 2. Binding Constants (K_b), Stern−Volmer Constants (K_{sv}) and the Apparent Binding Constants (K_{app}) for 1−6 and AVBH with ct-DNA, EB-ct-DNA, and DAPI-ct-DNA

compound	ct-DNA K_b, 10^4 M^{-1}	EB-ct-DNA K_{sv}, 10^4 M^{-1}	EB-ct-DNA K_{app} 10^5 M^{-1}	DAPI-ct-DNA K_{sv}, 10^4 M^{-1}
1	13.04 ± 0.41	2.52 ± 0.04	12.6	33.81 ± 0.18
2	10.50 ± 0.21	4.36 ± 0.07	21.8	27.05 ± 0.06
3	1.52 ± 0.12	1.70 ± 0.08	8.5	22.51 ± 0.07
4	1.71 ± 0.04	1.73 ± 0.07	8.65	11.50 ± 0.04
5	1.65 ± 0.03	1.66 ± 0.04	8.3	17.68 ± 0.09
6	1.43 ± 0.06	1.74 ± 0.09	8.7	22.93 ± 0.11
AVBH	4.36 ± 0.12	0.54 ± 0.06	2.7	4.85 ± 0.62

Table 3. Protein Quenching Constants (K_{sv}), Binding Constants (K_b), and Numbers of Binding Sites (n) for the Interaction of 1−6 and AVB with BSA

compound	K_{sv}, 10^5 M^{-1}	K_q, 10^{13} M^{-1}	K_b, 10^5 M^{-1}	n
1	2.75 ± 0.09	4.43 ± 0.01	54.95 ± 1.22	1.24 ± 0.02
2	2.49 ± 0.08	4.01 ± 0.01	38.72 ± 2.35	1.27 ± 0.03
3	0.89 ± 0.01	1.43 ± 0.02	0.99 ± 0.34	1.10 ± 0.02
4	0.78 ± 0.03	1.25 ± 0.01	0.11 ± 0.02	0.80 ± 0.02
5	0.96 ± 0.02	1.54 ± 0.02	0.57 ± 0.12	0.92 ± 0.03
6	1.18 ± 0.06	1.90 ± 0.01	0.91 ± 0.06	1.06 ± 0.05
AVBH	7.42 ± 0.37	11.97 ± 0.06	96.38 ± 0.21	1.04 ± 0.09

(excitation wavelength at 285 nm) was monitored after addition of increasing concentrations of **1−6** or AVBH. The values of K_{sv}, K_q, and K_b (Table 3 and Figure S14 in the Supporting Information) indicate that free AVBH has the highest affinity for BSA, and **1** and **2** show a slightly higher affinity in comparison to **3−6**.

The values of the bimolecular quenching constant (K_q) fall in the range (1.25−11.9) × 10^{13} L mol^{-1} s^{-1}, higher than the maximum possible value for dynamic quenching (2.0 × 10^{10} L mol^{-1} s^{-1}),[68] suggesting the involvement of a static quenching mechanism for **1−6**. For all complexes, the estimated values of n (∼1) support the likelihood of a single binding site in BSA for both AVBH and **1−6**. The higher binding affinities observed for compounds **1** and **2** correlate with the instability of these two complexes, releasing free AVBH, which can easily be bound by a cysteine residue of the protein.

Given the lower affinity for DNA and BSA binding but higher cytotoxic activity of the mono- and dicationic in comparison to the neutral complexes, the cytotoxic effects of **3−6** are more likely driven by the increased water solubility and hence higher bioavailability of these compounds.

CONCLUSIONS

We have successfully prepared some novel ruthenium(II) arene derivatives with avobenzone and ancillary PTA and PTA-Me ligands conforming to three structural typologies: i.e., neutral [Ru(arene)(AVB)Cl], monocationic [Ru(arene)(AVB)(PTA)]$^+$, and dicationic [Ru(arene)(AVB)(PTA-Me)]$^{2+}$. The ionic complexes **3−6**, containing PTA and PTA-Me ligands, display a potent cytotoxicity in vitro against ovarian carcinoma (A2780 and A2780R) cell lines, higher than that of the neutral complexes **1** and **2**. This work gives a first insight into mechanistic studies on DNA and protein binding which show that attaching AVBH to the ruthenium(II) arene complex strongly increases the ability to bind DNA but decreases the affinity for BSA protein binding, two observations that correlate with the stability of the complexes. Further studies on target identification are required, however, to explain the high cytotoxicity of the stable cationic ruthenium compounds over the neutral complexes.

EXPERIMENTAL SECTION

Materials and Methods. The dimers [(arene)$RuCl_2$]$_2$ (arene = *p*-cym and hmb) were purchased from Aldrich, and avobenzone was purchased from TCI Europe and used as received. [PTA-Me][BF_4] was synthesized as previously described.[69] All other materials were obtained from commercial sources and were used as received. IR spectra were recorded from 4000 to 30 cm^{-1} on a PerkinElmer Frontier FT-IR/FIR spectrometer. ^{1}H and ^{13}C NMR spectra were recorded on a Varian 400 Mercury Plus instrument operating at room temperature (400 MHz for ^{1}H, 100 MHz for ^{13}C) relative to TMS. ^{31}P NMR spectra were recorded on a Varian 400 Mercury Plus instrument operating at room temperature, 162 MHz relative to 85% H_3PO_4. Coupling constants are in Hz. Abbreviations: s, singlet; d, doublet; sept, septet; m, complex multiplet; vt, virtual triplet; br, broad. Positive and negative ion electrospray ionization mass spectra (ESI-MS) were obtained on a Series 1100 MSI detector HP spectrometer using methanol as the mobile phase. Solutions for analysis (3 mg/mL) were prepared using reagent-grade methanol. Masses and intensities were compared to those calculated using an IsoPro Isotopic Abundance Simulator, version 2.1.28. Melting points are uncorrected and were recorded on a STMP3 Stuart scientific instrument and on a capillary apparatus. Samples for microanalysis were dried in vacuo to constant weight (20 °C, ca. 0.1 Torr) and analyzed on a Fisons Instruments 1108 CHNS-O elemental analyzer. Electrical conductivity measurements (Λ_M, reported as S cm^2 mol^{-1}) of acetonitrile solutions of the complexes were recorded using a Eutech Instruments CON2700 apparatus at room temperature. UV−vis spectra of the proligands and complexes were measured with a Varian Cary1 spectrometer at 20 °C. The fluorescence of the proligands and complexes was analyzed using a Hitachi F-4500 spectrofluorimeter at 20 °C.

Synthesis of the Ruthenium Complexes. *[(cym)Ru(AVB)Cl] (**1**).* Avobenzone (285.6 mg, 0.92 mmol) was dissolved in methanol (20 mL), and KOH (52.0 mg, 0,92 mmol) was added. The mixture was stirred for 1 h at room temperature, and then [(cym)$RuCl_2$]$_2$ (244.9 mg, 0.40 mmol) was added. The mixture was stirred for 24 h at room temperature, and an orange precipitate formed, which was removed by filtration and washed with *n*-hexane (372.6 mg, 0.64 mmol, yield 80%). The residue was concentrated to ca. 2 mL and stored at 4 °C. Red crystals formed over several days. Compound **1** is soluble in alcohols, acetone, acetonitrile, chlorinated solvents, DMF, and DMSO and

DOI: 10.1021/acs.organomet.6b00694
Organometallics XXXX, XXX, XXX−XXX

slightly soluble in diethyl ether. Mp: 220−221 °C. Anal. Calcd for $C_{30}H_{35}ClO_3Ru$: C, 62.11; H, 6.08. Found: C, 62.37; H, 6.04. IR (cm^{-1}): 3066−2838 w ν(C−H), 1605 m, 1588 m, 1532 vs ν(C═O; C═C), 1377 s, 1253 s, 1180 s, 1034 s, 836 s, 781 vs, 648 m, 274 s ν(Ru−Cl). ^{1}H NMR ($CDCl_3$, 293 K): δ, 1.31 (s, 9H, C-(CH_3)$_3$ of AVB), 1.36 (d, 6H, $CH_3C_6H_4CH(CH_3)_2$, J = 6.8 Hz), 2.32 (s, 3H, $CH_3C_6H_4CH(CH_3)_2$), 3.01 (sept, 1H, $CH_3C_6H_4CH(CH_3)_2$, J = 6.8 Hz), 3.83 (s, 3H, OCH_3 of AVB), 5.28 (d, 2H, $CH_3C_6H_4CH(CH_3)_2$, J = 6.0 Hz), 5.56 (m, 2H, $CH_3C_6H_4CH(CH_3)_2$), 6.39 (s, 1H, C(7)H of AVB), 6.87 (d, 2H, C(3,3′)H of AVB, J = 9.2 Hz), 7.38 (d, 2H, C(11,11′)H of AVB, J = 8.4 Hz), 7.83 (d, 2H, C(10,10′)H of AVB, J = 8.4 Hz), 7.88 (d, 2H, C(4,4′)H of AVB, J = 9.2 Hz). ^{13}C[^{1}H] NMR ($CDCl_3$, 293 K): δ 18.1 (s, $CH_3C_6H_4CH(CH_3)_2$), 22.6 (s, $CH_3C_6H_4CH(CH_3)_2$), 31.1 (s, $CH_3C_6H_4CH(CH_3)_2$), 31.4 (s, C-(CH_3)$_3$ of AVB), 35.1 (s, C-(CH_3)$_3$ of AVB), 55.5 (s, OCH_3 of AVB), 79.6, 83.3 (s, $CH_3C_6H_4CH(CH_3)_2$), 92.7 (s, C(7) of AVB), 97.4, 99.9 (s, $CH_3C_6H_4CH(CH_3)_2$), 113.6 (s, C(3,3′) of AVB), 125.2 (s, C(11,11′) of AVB), 127.3 (s, C(10,10′) of AVB), 129.3 (s, C(4,4′) of AVB), 131.9 (s, C(5) of AVB), 136.7 (s, C(9) of AVB), 154.4 (s, C(12) of AVB), 162.2 (s, C(2) of AVB), 180.7 (s, C(8) of AVB), 181.2 (s, C(6) of AVB). ESI-MS (+) CH_3OH (m/z [relative intensity, %]): 545 [100] [(cym)Ru(AVB)]$^+$. Λ_m (CH_3CN, 293 K, 10^{-4} mol/L): 28 S cm^2 mol^{-1}.

*[(hmb)Ru(AVB)Cl] (**2**).* Avobenzone (249.9 mg, 0.81 mmol) was dissolved in methanol (30 mL), and KOH (45.2 mg, 0.81 mmol)) was added. The mixture was stirred for 1 h at room temperature, and then [(hmb)$RuCl_2$]$_2$ (234.0 mg, 0.35 mmol) was added. The resulting mixture was stirred for 24 h at room temperature. The solvent was removed under reduced pressure, dichloromethane (10 mL) was added, and the mixture was filtered to remove the KCl precipitate. The solution was concentrated to 2 mL, and then addition of an excess of n-hexane resulted in precipitation of an orange powder (315.0 mg, 0.52 mmol, yield 74%). Compound **2** is soluble in alcohols, acetone, acetonitrile, chlorinated solvents, DMF, and DMSO and slightly soluble in diethyl ether. Mp: 261−263 °C. Anal. Calcd for $C_{32}H_{39}ClO_3Ru$: C, 63.20; H, 6.46. Found: C, 63.02; H, 6.41. IR (cm^{-1}): 3066−2838 w ν(C−H), 1604 m, 1589 m, 1532 vs, 1494 vs ν(C═O; C═C), 1422 s, 1349 s, 1255 s, 1180 s, 1035 s, 844 s, 787 vs, 625 m, 549 m, 516 m, 279 s ν(Ru−Cl). ^{1}H NMR ($CDCl_3$, 293 K): δ, 1.33 (s, 9H, C-(CH_3)$_3$ of AVB), 2.15 (s, 18H, CH_3(hmb)), 3.85 (s, 3H, OCH_3 of AVB), 6.40 (s, 1H, C(7)H of AVB), 6.88 (d, 2H, C(3,3′)H of AVB, J = 8.8 Hz), 7.39 (d, 2H, C(11,11′)H of AVB, J = 8.4 Hz), 7.90 (d, 2H, C(10,10′)H of AVB, J = 8.4 Hz), 7.95 (d, 2H, C(4,4′)H of AVB, J = 8.8 Hz). ^{13}C[^{1}H] NMR ($CDCl_3$, 293 K): δ 15.4 (s, CH_3(hmb)), 31.4 (s, C-(CH_3)$_3$ of AVB), 35.0 (s, C-(CH_3)$_3$ of AVB), 55.5 (s, OCH_3 of AVB), 90.5 (s, C_6(hmb)), 92.1 (s, C(7) of AVB), 113.5 (s, C(3,3′) of AVB), 125.1 (s, C(11,11′) of AVB), 127.1 (s, C(10,10′) of AVB), 129.1 (s, C(4,4′) of AVB), 132.3 (s, C(5) of AVB), 137.0 (s, C(9) of AVB), 154.1 (C(12) of AVB), 161.9 (C(2) of AVB), 179.9 (C(8) of AVB), 180.4 (s, C(6) of AVB). ESI-MS (+) CH_3OH (m/z [relative intensity, %]): 573 [100] [(hmb)Ru(AVB)]$^+$. Λ_m (CH_3CN, 293 K, 10^{-4} mol/L): 22 S cm^2 mol^{-1}.

*[(cym)Ru(AVB)(PTA)][CF_3SO_3] (**3**).* Compound **1** (101.5 mg, 0.175 mmol) was dissolved in methanol (20 mL), and $AgCF_3SO_3$ (45.0 mg, 0.175 mmol) was added. The mixture was stirred for 1 h at room temperature and filtered to remove AgCl. PTA (PTA = 1,3,5-triaza-7-phosphaadamantane; 27.5 mg, 0.175 mmol) was then added to the filtrate, and the resulting mixture was stirred for 24 h at room temperature. Then the solution was dried by rotary evaporation and dichloromethane (2 mL) and an excess of n-hexane were added. The mixture was left at 4 °C until a yellow precipitate formed. The powder was recovered by filtration and air-dried. Compound **3** (110.2 mg, 0.09 mmol, yield 74%), is soluble in alcohols, acetone, acetonitrile, chlorinated solvents, DMF, and DMSO and slightly soluble in diethyl ether and water. Mp: 150−153 °C. Anal. Calcd for $C_{37}H_{47}F_3N_3O_6PRuS$: C, 52.23; H, 5.57; N, 4.94; S, 3.77. Found: C, 52.20; H, 5.62; N, 4.87; S, 3.73. IR (cm^{-1}): 3070−2962 m ν(C−H), 1603 m, 1584 m, 1524 vs ν(C═O; C═C), 1373 s, 1253 vs, 1152 s, 1029 vs ν(SO_3CF_3), 971 s, 946 vs, 786 s, 741 m, 637 s. ^{1}H NMR (CD_3CN, 293 K): δ, 1.31 (d, 6H, $CH_3C_6H_4CH(CH_3)_2$, J = 6.8 Hz), 1.37 (s, 9H, C(CH_3)$_3$ of AVB), 2.15 (s, 3H, $CH_3C_6H_4CH(CH_3)_2$), 2.71 (sept, 1H, $CH_3C_6H_4CH(CH_3)_2$, J = 6.8 Hz), 3.89 (s, 3H, OCH_3 of AVB), 4.13 (s, 6H, NCH_2P, PTA), 4.44 (s, 6H, NCH_2N, PTA), 5.86 (d, 2H, $CH_3C_6H_4CH(CH_3)_2$, J = 6.0 Hz), 5.91 (m, 2H, $CH_3C_6H_4CH(CH_3)_2$), 6.82 (s, 1H, C(7)H of AVB), 7.04 (d, 2H, C(3,3′)H of AVB, J = 9.2 Hz), 7.56 (d, 2H, C(11,11′)H of AVB, J = 8.4 Hz), 7.93 (d, 2H, C(10,10′)H of AVB, J = 8.4 Hz), 7.99 (d, 2H, C(4,4′)H of AVB, J = 9.2 Hz). ^{13}C[^{1}H] NMR (CD_3CN, 293 K): δ 17.4 (s, $CH_3C_6H_4CH(CH_3)_2$), 22.4 (s, $CH_3C_6H_4CH(CH_3)_2$), 31.3 (s, $CH_3C_6H_4CH(CH_3)_2$), 31.4 (s, C-(CH_3)$_3$ of AVB), 35.7 (s, C-(CH_3)$_3$ of AVB), 52.2 (d, PCH_2N, PTA, J_{CP} = 13.7 Hz), 56.4 (s, OCH_3 of AVB), 73.1 (d, NCH_2N, PTA, J_{CP} = 7.7 Hz), 89.3 and 90.6 (s, $CH_3C_6H_4CH(CH_3)_2$), 95.4 (s, C(7) of AVB), 98.4 and 105.3 (s, $CH_3C_6H_4CH(CH_3)_2$), 114.9 (s, C(3,3′) of AVB), 126.7 (s, C(11,11′) of AVB), 128.2 (s, C(10,10′) of AVB), 130.5 (s, C(4,4′) of AVB), 130.8 (s, C(5) of AVB), 135.9 (s, C(9) of AVB), 156.6 (s, C(12) of AVB), 164.0 (s, C(2) of AVB), 183.2 (s, C(8) of AVB), 183.3 (s, C(8) of AVB). ^{31}P[^{1}H] NMR (CD_3CN, 293 K): δ − 28.4 (s, PTA). ESI-MS (+) CH_3OH (m/z [relative intensity, %]): 702 [100] [(cym)Ru-(AVB)(PTA)]$^+$, 545 [5] [(cym)Ru(AVB)]$^+$. Λ_m (CH_3CN, 293 K, 10^{-4} mol/L): 101 S cm^2 mol^{-1}.

*[(hmb)Ru(AVB)(PTA)][CF_3SO_3] (**4**).* Compound **4** was prepared following a procedure similar to that reported for **3** by using precursor **2** (84.0 mg, 0.095 mmol, yield 74%). Compound **4** is soluble in alcohols, acetone, acetonitrile, chlorinated solvents, DMF, and DMSO and slightly soluble in diethyl ether and water. Mp: 200−202 °C. Anal. Calcd for $C_{39}H_{51}F_3N_3O_6PRuS$: C, 53.29; H, 5.85; N, 4.78; S, 3.65. Found: C, 53.18; H, 5.83; N, 4.70; S, 3.57. IR (cm^{-1}): 2959 br ν(C−H), 1603 m, 1583 m, 1523 vs ν(C═O; C═C), 1258 vs, 1175 m, 1030 vs ν(SO_3CF_3), 972 s, 947 vs, 787 s, 637 s, 573 m. ^{1}H NMR ($CDCl_3$, 293 K): δ, 1.37 (s, 9H, C-(CH_3)$_3$ of AVB), 2.16 (s, 18H, CH_3(hmb)), 3.90 (s, 3H, OCH_3 of AVB), 4.11 (s, 6H, NCH_2P, PTA), 4.50 (s, 6H, NCH_2N, PTA), 6.71 (s, 1H, C(7)H of AVB), 7.00 (d, 2H, C(3,3′)H of AVB, J = 8.8 Hz), 7.49 (d, 2H, C(11,11′)H of AVB, J = 8.4 Hz), 7.86 (d, 2H, C(10,10′)H of AVB, J = 8.4 Hz), 7.93 (d, 2H, C(4,4′)H of AVB, J = 8.8 Hz). ^{13}C[^{1}H] NMR ($CDCl_3$, 293 K): δ 16.1 (s, CH_3(hmb)), 31.4 (s, C-(CH_3)$_3$ of AVB), 35.3 (s, C-(CH_3)$_3$ of AVB), 49.7 (d, PCH_2N, PTA, J_{CP} = 12.2 Hz), 55.8 (OCH_3 of AVB), 73.0 (d, NCH_2N, PTA, J_{CP} = 6.8 Hz),), 93.7 (s, C_6(hmb)), 98.5, (s, C(7) of AVB), 114.5 (s, C(3,3′) of AVB), 126.1 (s, C(11,11′) of AVB), 126.8 (s, C(10,10′) of AVB), 129.1 (s, C(4,4′) of AVB), 130.4 (s, C(5) of AVB), 135.3 (s, C(9) of AVB), 156.1 (s, C(12) of AVB), 163.4 (s, C(2) of AVB), 181.8 (s, C(6,8) of AVB). ^{31}P[^{1}H] NMR ($CHCl_3$, 293 K): δ − 34.0 (s, PTA). ESI-MS (+) CH_3OH (m/z [relative intensity, %]): 730 [100] [(hmb)Ru(AVB)(PTA)]$^+$, 573 [5] [(hmb)Ru-(AVB)]$^+$. Λ_m (CH_3CN, 293 K, 10^{-4} mol/L): 113 S cm^2 mol^{-1}.

*[(cym)Ru(AVB)(PTA-Me)][BF_4][CF_3SO_3] (**5**).* Compound **5** was prepared following a procedure similar to that reported for **3** by using [PTA-Me][BF_4] (1-methyl-1-azonia-3,5-diaza-7-phosphatricyclo[3.3.1.1]decane tetrafluoroborate) (67.8 mg, 0.07 mmol, yield 70%). Compound **5** is soluble in alcohols, acetone, acetonitrile, chlorinated solvents, DMF, and DMSO and slightly soluble in water. Mp: 159−161 °C. Anal. Calcd for $C_{38}H_{50}BF_7N_3O_6PRuS$: C, 47.91; H, 5.29; N, 4.41; S, 3.37. Found: C, 47.76; H, 5.33; N, 4.35; S, 3.31. IR (cm^{-1}): 3611−2966 m ν(C−H), 1604 m, 1584 m, 1524 s ν(C═O; C═C), 1360 m, 1251 s, 1175 s, 1029 vs ν(SO_3CF_3), 791 m, 750 s, 638 vs, 573 s, 550 m, 518 s. ^{1}H NMR (CD_3CN, 293 K): δ, 1.32 (d, 6H, $CH_3C_6H_4CH(CH_3)_2$, J = 6.8 Hz), 1.37 (s, 9H, C(CH_3)$_3$ of AVB), 2.17 (s, 3H, $CH_3C_6H_4CH(CH_3)_2$), 2.71 (s, 3H, N^+CH_3), 2.75 (sept, 1H, $CH_3C_6H_4CH(CH_3)_2$, J = 6.8 Hz), 4.04 and 4.17 ($J(H^AH^B)$ = 15.0 Hz, $^2J(H^A$-P) = 15 Hz, $^2J(H^B$-P) = 5 Hz, 4H, PCH^AH^BN, PTA-Me), 3.91 (s, 3H, OCH_3 of AVB), 4.38 (s, 2H, PCH_2N^+, PTA-Me), 4.36 and 4.52 ($J(H^AH^B)$ = 15 Hz, 2H, NCH^AH^BN, PTA-Me), 4.81 and 4.97 ($J(H^AH^B)$ = 13 Hz, 4H, $NCH^AH^BN^+$, PTA-Me), 6.02 (m, 2H, $CH_3C_6H_4CH(CH_3)_2$), 6.06 (m, 2H, $CH_3C_6H_4CH(CH_3)_2$), 6.87 (s, 1H, C(7)H of AVB), 7.05 (d, 2H, C(3,3′)H of AVB, J = 8.8 Hz), 7.58 (d, 2H, C(11,11′)H of AVB, J = 8.4 Hz), 7.97 (d, 2H, C(10,10′)H of AVB, J = 8.4 Hz), 8.03 (d, 2H, C(4,4′)H of AVB, J = 8.8 Hz). ^{13}C[^{1}H] NMR ($CDCl_3$, 293 K): δ 18.7 (s, $CH_3C_6H_4CH(CH_3)_2$), 22.5 (s, $CH_3C_6H_4CH(CH_3)_2$), 30.9 (s,

DOI: 10.1021/acs.organomet.6b00694
Organometallics XXXX, XXX, XXX−XXX

$CH_3C_6H_4CH(CH_3)_2$), 31.3 (s, C-(CH_3)$_3$ of AVB), 35.4 (s, *C*-(CH_3)$_3$ of AVB), 47.0 (dd, vt, $^1J_{CP}$ = 15.7 Hz, PCH_2N, PTA-Me), 49.2 (s, N^+CH_3, PTA-Me), 55.9 (OCH_3 of AVB), 58.7 (s, PCH_2N^+, PTA-Me), 70.2 (s, NCH_2N, PTA-Me) 80.8 (s, NCH_2N^+, PTA-Me), 88.3, 89.0, 90.3, 90.7 (s, $CH_3C_6H_4CH(CH_3)_2$), 94.4 (s, *C*(7) of AVB), 99.9 and 107.1 (s, $CH_3C_6H_4CH(CH_3)_2$), 114.6 (s, *C*(3,3′) of AVB), 126.3 (s, *C*(11,11′) of AVB), 127.2 (s, *C*(10,10′) of AVB), 129.1 (s, *C*(5) of AVB), 129.6 (s, *C*(4,4′) of AVB), 134.1 (s, *C*(9) of AVB), 156.7 (s, *C*(12) of AVB), 163.6 (s, *C*(2) of AVB), 182.7 (s, *C*(6,8) of AVB). $^{31}P[^1H]$ NMR ($CDCl_3$, 293 K): δ, −13.2. ESI-MS (+) CH_3OH (*m*/*z* [relative intensity, %]): 545 [100] [(cym)Ru(AVB)]$^+$, 172 [45] [PTA-Me]$^+$. Λ_m (CH_3CN, 293 K, 10^{-4} mol/L): 262 S cm^2 mol^{-1}.

*[(hmb)Ru(AVB)(PTA-Me)][BF$_4$][CF$_3$SO$_3$] (**6**).* Compound **6** was prepared following a procedure similar to that reported for **4** by using [PTA-Me][BF_4] (61.2 mg, 0.06 mmol, yield 61%). Compound **6** is soluble in alcohols, acetone, acetonitrile, chlorinated solvents, DMF, and DMSO and slightly soluble in water. Mp: 208−210 °C. Anal. Calcd for $C_{40}H_{54}BF_7N_3O_6PRuS$: C, 48.99; H, 5.55; N, 4.28; S, 3.27. Found: C, 49.10; H, 5.65; N, 4.36; S, 3.33. IR (cm^{-1}): 3610−2962 w ν(C−H), 1603 m, 1583 m, 1523 s ν(C═O; C═C), 1356 m, 1252 vs, 1175 s, 1023 vs $\nu(SO_3CF_3)$, 814 m, 790 m, 750 m, 638 vs, 572 s, 551 m, 518 s. ^{1}H NMR (CD_3CN, 293 K): δ, 1.37 (s, 9H, C-(CH_3)$_3$ of AVB), 2.18 (s, 18H, CH_3, hmb), 2.64 (s, 3H, N^+CH_3), 3.92 (s, 3H, OCH_3 of AVB), 3.92 and 4.22 ($J(H^AH^B)$ = 15.0 Hz, $^2J(H^A$-P) = 5 Hz, $^2J(H^B$-P) = 0, 4H, PCH^AH^BN, PTA-Me), 4.04 (s, 2H, PCH_2N^+, PTA-Me), 4.36 and 4.49 ($J(H^AH^B)$ = 12 Hz, 2H, NCH^AH^BN, PTA-Me), 4.75 and 4.82 ($J(H^AH^B)$ = 12 Hz, 4H, $NCH^AH^BN^+$, PTA-Me), 6.90 (s, 1H, C(7)*H* of AVB), 7.07 (d, 2H, C(3,3′)*H* of AVB, *J* = 8.8 Hz), 7.59 (d, 2H, C(11,11′)*H* of AVB, *J* = 8.4 Hz), 8.04 (d, 2H, C(10,10′)*H* of AVB, *J* = 8.8 Hz), 8.10 (d, 2H, C(4,4′)*H* of AVB, *J* = 8.8 Hz). $^{13}C[^1H]$ NMR ($CDCl_3$, 293 K): δ 15.9 (CH_3(hmb)), 31.3 (C(CH_3)$_3$ of AVB), 35.3 (*C*(CH_3)$_3$ of AVB), 45.6 (d, $^1J_{CP}$ = 25.4 Hz, PCH_2N, PTA-Me), 49.2 (s, N^+CH_3, PTA-Me), 54.6, (d, $^1J_{CP}$ = 19.3 Hz, PCH_2N^+, PTA-Me), 55.8 (s, OCH_3 of AVB), 69.8 (s, NCH_2N, PTA-Me), 80.8 (s, NCH_2N^+, PTA-Me), 93.5 (C_6(hmb)), 99.6 (s, *C*(7) of AVB), 114.6 (s, *C*(3,3′) of AVB), 126.2 (s, *C*(11,11′) of AVB), 127.0 (s, *C*(10,10′) of AVB), 129.4 (s, *C*(5) of AVB), 129.9 (s, *C*(4,4′) of AVB), 134.8 (s, *C*(9) of AVB), 156.5 (s, *C*(12) of AVB), 163.6 (s, *C*(2) of AVB), 181.9 (s, *C*(6,8) of AVB).$^{31}P[^1H]$ NMR ($CDCl_3$, 293 K): δ, −18.6. ESI-MS (+) CH_3OH (*m*/*z* [relative intensity, %]): 573 [55] [(cym)Ru-(AVB)]$^+$, 172 [100] [PTA-Me]$^+$. Λ_m (CH_3CN, 293 K, 10^{-4} mol/L): 192 S cm^2 mol^{-1}.

X-ray Crystallography. Diffraction data were recorded at low temperature (100(2) K) using Mo Kα radiation on a Bruker APEX II CCD diffractometer equipped with a κ geometry goniometer. The data sets were reduced by EvalCCD[70] and then corrected for absorption.[71] The solutions and refinements were performed by SHELX.[72] The crystal structures were refined using full-matrix least squares based on F^2 with all non-hydrogen atoms anisotropically defined. Hydrogen atoms were placed in calculated positions by means of the "riding" model. In the crystal structure of **2**, one of the two independent molecules displayed, during the last stages of refinement, disorder problems (*tert*-butyl and −OMe substituents may occupy the same position). In order to handle these problems correctly and to retain a reasonable geometry and acceptable ADPs, a split model, in combination with some soft restraints (SIMU and SADI cards), was employed. A very small twinning (TWIN 100, 0−10, 00−1) component was found for **2**, and its refined BASF parameter was 0.0189(6).

Cell Culture and Inhibition of Cell Growth. The human A2780 and A2780cisR ovarian carcinoma and HEK293 (human embryonic kidney) cells were obtained from the European Collection of Cell Cultures (Salisbury, U.K.). A2780 and A2780cisR cells were grown routinely in RPMI-1640 medium, while HEK293 cells were grown in DMEM medium, with 10% fetal bovine serum (FBS) and 1% antibiotics at 37 °C and 5% CO_2. Cytotoxicity was determined using the MTT assay (MTT = 3-(4,5-dimethyl-2-thiazolyl)-2,5-diphenyl-2*H*-tetrazolium·bromide). Cells were seeded in 96-well plates as monolayers with 100 μL of cell suspension (approximately 10000 cells) per well and preincubated for 24 h in medium supplemented with 10% FBS. Compounds were prepared as DMSO solutions and then dissolved in the culture medium and serially diluted to the appropriate concentration, to give a final DMSO concentration of 0.5%. A 100 μL portion of the drug solution was added to each well, and the plates were incubated for another 72 h. Subsequently, MTT (5 mg/mL solution) was added to the cells and the plates were incubated for a further 2 h. The culture medium was aspirated, and the purple formazan crystals formed by the mitochondrial dehydrogenase activity of vital cells were dissolved in DMSO. The optical density, directly proportional to the number of surviving cells, was quantified at 590 nm using a multiwell plate reader, and the fraction of surviving cells was calculated from the absorbance of untreated control cells. Evaluation is based on means from at least two independent experiments, each comprising quadruplicates per concentration level.

DNA Interaction Studies. Stock solutions of calf thymus DNA (ct-DNA) (Sigma-Aldrich) were prepared by dissolving the DNA powder overnight in 20 mM phosphate buffer pH 7.4 containing 5 mM NaCl and incubated with stirring at 4 °C for 12 h. The UV absorbance at 260 and 280 nm of the DNA solution gave an A260/A280 solution ratio of ct-DNA of ca. 1.9, indicating that the DNA was sufficiently free from protein.[68] The concentration of ct-DNA solution was determined by UV absorbance at 260 nm. The molar absorption coefficient, ε_{260}, was taken as 6600 M^{-1} cm^{-1}.[73] All AVB complexes and ligands were dissolved in DMSO. Electronic absorption titrations of different complexes with DNA were recorded at 25 °C by addition of ct-DNA in small aliquots (from 0 to 63 μM) to buffer solution (50 mM phosphate buffer pH 7.4) containing the complexes **1**−**6** or AVBH.. Absorption spectra were recorded from 200 to 600 nm, and changes on the intensity of the bands were monitored. The intrinsic binding constant K_b for the interaction of **1**−**6** or AVBH with ct-DNA was determined from a plot of [DNA]/(ε_a − ε_f) versus [DNA], by using absorption spectral titration data and eq 1:

$$[DNA]/|\varepsilon_a - \varepsilon_f| = [DNA]/|\varepsilon_b - \varepsilon_f| + 1/K_b|\varepsilon_b - \varepsilon_f| \quad (1)$$

where [DNA] is the concentration of DNA, the apparent absorption coefficients ε_a, ε_f, and ε_b correspond to A_{obsd}/[complex], the extinction coefficient for the free metal complex, and the extinction coefficient for the metal complex in the fully bound form, respectively.[73] The K_b value is given by the ratio of the slope to the intercept.

Major Groove Displacement Assay. Competitive binding experiments were performed with the ethidium bromide (EB) and ct-DNA concentrations maintained at 5 and 55.7 μM, respectively, while the concentrations of different complexes added to the buffer solution were increased. Fluorescence quenching spectra were recorded using a Hitachi 4500 spectrofluorimeter with an excitation wavelength of 490 nm and emission spectrum of 500−700 nm. The fluorescence spectra were recorded, and the fluorescence values of decrease in emission spectra were corrected according to the relationship given by eq 2:

$$F_c = F_m \times e^{(A1+A2)/2} \quad (2)$$

where F_c and F_m are the corrected and measured fluorescences, respectively. A1 and A2 are the absorbances of the tested compounds at the excitation and emission wavelengths. For fluorescence quenching experiments, the Stern−Volmer equation was used (eq 3):

$$F_0/F_c = 1 + k_q\tau_0[C] = 1 + K_{sv}[C] \quad (3)$$

where F_0 and F_c represent the fluorescence intensities in the absence and in the presence of the metal complex, respecitvely, [C] is the concentration of the metal complex, and K_{sv} is the Stern−Volmer constant that can be obtained from fluorescence data, plotted as F_0/F_c vs the metal complex concentration [C].[74] All experiments involving ct-DNA were performed in buffer solution (50 mM phosphate buffer pH 7.4) at room temperature. The apparent binding constant K_{app} of AVBH and **1**−**6** was calculated from eq 4:

$$K_{EB}[EB] = K_{app}[C] \quad (4)$$

DOI: 10.1021/acs.organomet.6b00694
Organometallics XXXX, XXX, XXX−XXX

where K_{EB} and [EB] are the binding constant and concentration of EB, respectively, and [C] is the concentration of the metal complex at 50% reduction of fluorescence.[75]

Minor Groove Displacement Assay. Samples were prepared in triplicate for each concentration, and at least seven different concentrations were used. In a typical experiment, the changes in the emission spectra of the DAPI complex with the DNA in 50 mM phosphate buffer pH 7.4 were monitored upon addition of increasing concentrations of AVB and complexes at room temperature. Fluorescence quenching data were evaluated after excitation of the DAPI-ct-DNA complex at 338 nm and recording of the spectra from 400 to 600 nm. Values of K_{sv} constants were evaluated using eq 3, and the quenching fluorescence values obtained were corrected according to the relationship given by eq 2.

BSA Binding Studies. The protein-binding studies were performed by tryptophan fluorescence quenching experiments using bovine serum albumin (BSA) prepared in 50 mM potassium phosphate buffer pH 7.4. Fluorescence measurements were recorded on a Hitachi 4500 spectrofluorometer with the concentration of BSA kept constant (15×10^{-6} M) while increasing complex concentrations were added to the protein solution at room temperature. Protein fluorescence intensities were recorded after each successive addition of complex solution and equilibration (ca. 5 min). Fluorescence spectra were recorded from 300 to 450 nm at an excitation wavelength of 285 nm. The values of Stern−Volmer constants of the different metal complexes to HSA were evaluated following eq 3 ,and fluorescence values were corrected by eq 2. K_{sv}, the Stern−Volmer quenching constant, was determined by linear regression of a plot of F_0/F vs [C]; K_q is the bimolecular quenching rate constant, and τ_0 is the average fluorescence lifetime of the fluorophore in the absence of drug, having a value of 6.2 ns for the biopolymer.[76] Considering the existence of similar and independent binding sites in the BSA for the static quenching interaction, the binding constant (K_b) and the number of the binding sites (n) for the different complexes on BSA can be determined according to eq 5:[77]

$$\log[(F_0 - F)/F] = \log K_b + n \log[Q] \quad (5)$$

where, in the present case, K_b is the binding constant for the complex−protein interaction and n is the number of binding sites per albumin molecule. Values of K_b and n can be determined by the slope and the intercept of the double-logarithm regression curve of $\log[(F_0 - F)/F]$ versus log[C].

■ ASSOCIATED CONTENT

Supporting Information

The Supporting Information is available free of charge on the ACS Publications website at DOI: 10.1021/acs.organomet.6b00694.

NMR, absorption, emission, and fluorescence spectra and crystal data (PDF)
Crystallographic data (CIF)
Crystallographic data (CIF)

■ AUTHOR INFORMATION

Corresponding Authors

*R.P.: e-mail, riccardo.pettinari@unicam.it; tel. +39 0737402338.
*P.D.: e-mail, paul.dyson@epfl.ch.

Notes

The authors declare no competing financial interest.

■ ACKNOWLEDGMENTS

We thank the Swiss National Science Foundation, EPFL, the University of Camerino, and the NCN program (Grant No. 2012/07/B/ST/00885) of Poland for financial support.

■ REFERENCES

(1) Singh, S. K.; Pandey, D. S. Multifaceted half-sandwich arene-ruthenium complexes: Interactions with biomolecules, photoactivation, and multinuclearity approach. *RSC Adv.* **2014**, *4*, 1819−1840.
(2) Sava, G.; Bergamo, A.; Dyson, P. J. Metal-based antitumour drugs in the post-genomic era: What comes next? *Dalton Trans.* **2011**, *40*, 9069−9075.
(3) Meggers, E. From conventional to unusual enyzme inhibitor scaffolds: The quest for target specificity. *Angew. Chem., Int. Ed.* **2011**, *50*, 2442−2448.
(4) Smith, G. S.; Therrien, B. Targeted and multifunctional arene ruthenium chemotherapeutics. *Dalton Trans.* **2011**, *40*, 10793−10800.
(5) Gasser, G.; Ott, I.; Metzler-Nolte, N. Organometallic anticancer compounds. *J. Med. Chem.* **2011**, *54*, 3−25.
(6) Noffke, A. L.; Habtemariam, A.; Pizarro, A. M.; Sadler, P. J. Designing organometallic compounds for catalysis and therapy. *Chem. Commun.* **2012**, *48*, 5219−5246.
(7) Barry, N. P. E.; Sadler, P. J. Exploration of the medical periodic table: Towards new targets. *Chem. Commun.* **2013**, *49*, 5106−5131.
(8) Hartinger, C. G.; Groessl, M.; Meier, S. M.; Casini, A.; Dyson, P. J. Application of mass spectrometric techniques to delineate the modes-of-action of anticancer metallodrugs. *Chem. Soc. Rev.* **2013**, *42*, 6186−6199.
(9) Rademaker-Lakhai, J. M.; van den Bongard, D.; Pluim, D.; Beijnen, J. H.; Schellens, J. H. A phase I and pharmacological study with imidazolium-trans-DMSO-imidazole-tetrachlororuthenate, a novel ruthenium anticancer agent. *Clin. Cancer Res.* **2004**, *10*, 3717−3727.
(10) Hartinger, C. G.; Jakupec, M. A.; Zorbas-Seifried, S.; Groessl, M.; Egger, A.; Berger, W.; Zorbas, H.; Dyson, P. J.; Keppler, B. K. KP1019, A New Redox-Active Anticancer Agent−Preclinical Development and Results of a Clinical Phase I Study in Tumor Patients. *Chem. Biodiversity* **2008**, *5*, 2140−2155.
(11) Trondl, R.; Heffeter, P.; Kowol, C. R.; Jakupec, M. A.; Berger, W.; Keppler, B. K. NKP-1339, the first ruthenium-based anticancer drug on the edge to clinical application. *Chem. Sci.* **2014**, *5*, 2925−2932.
(12) Yan, Y. K.; Melchart, M.; Habtemariam, A.; Sadler, P. J. Organometallic chemistry, biology and medicine: Ruthenium arene anticancer complexes. *Chem. Commun.* **2005**, 4764−4776.
(13) Ang, W. H.; Casini, A.; Sava, G.; Dyson, P. J. Organometallic ruthenium-based antitumor compounds with novel modes of action. *J. Organomet. Chem.* **2011**, *696*, 989−998.
(14) Therrien, B. Functionalised η6-arene ruthenium complexes. *Coord. Chem. Rev.* **2009**, *253*, 493−519.
(15) Nováková, O.; Nazarov, A. A.; Hartinger, C. G.; Keppler, B. K.; Brabec, V. DNA interactions of dinuclear RuII arene antitumor complexes in cell-free media. *Biochem. Pharmacol.* **2009**, *77*, 364−374.
(16) Hartinger, C. G.; Zorbas-Seifried, S.; Jakupec, M. A.; Kynast, B.; Zorbas, H.; Keppler, B. K. From bench to bedside - preclinical and early clinical development of the anticancer agent indazolium trans-[tetrachlorobis(1H-indazole)ruthenate(III)] (KP1019 or FFC14A). *J. Inorg. Biochem.* **2006**, *100*, 891−904.
(17) Pacor, S.; Zorzet, S.; Cocchietto, M.; Bacac, M.; Vadori, M.; Turrin, C.; Gava, B.; Castellarin, A.; Sava, G. Intratumoral NAMI-A treatment triggers metastasis reduction, which correlates to CD44 regulation and tumor infiltrating lymphocyte recruitment. *J. Pharmacol. Exp. Ther.* **2004**, *310*, 737−744.
(18) Sava, G.; Zorzet, S.; Turrin, C.; Vita, F.; Soranzo, M.; Zabucchi, G.; Cocchietto, M. Bergamo, A.; DiGiovine, S.; Pezzoni, G., Dual Action of NAMI-A in Inhibition of Solid Tumor Metastasis Selective Targeting of Metastatic Cells and Binding to Collagen. *Clin. Cancer Res.* **2003**, *9*, 1898−1905.
(19) Bergamo, A.; Riedel, T.; Dyson, P. J.; Sava, G. Preclinical combination therapy of the investigational drug NAMI-A+ with doxorubicin for mammary cancer. *Invest. New Drugs* **2015**, *33*, 53−63.
(20) Leijen, S.; Burgers, S. A.; Baas, P.; Pluim, D.; Tibben, M.; Werkhoven, E.; Alessio, E.; Sava, G.; Beijnen, J. H.; Schellens, J. H. M. Phase I/II study with ruthenium compound NAMI-A and gemcitabine

DOI: 10.1021/acs.organomet.6b00694
Organometallics XXXX, XXX, XXX−XXX

in patients with non-small cell lung cancer after first line therapy. *Invest. New Drugs* **2015**, *33*, 201−214.
(21) Allardyce, C. S.; Dyson, P. J.; Ellis, D. J.; Heath, S. L. [Ru(η6-p-cymene)Cl2(pta)] (pta = 1,3,5-triaza-7-phosphatricyclo-[3.3.1.1]-decane): A water soluble compound that exhibits pH dependent DNA binding providing selectivity for diseased cells. *Chem. Commun.* **2001**, 1396−1397.
(22) Ang, W. H.; Daldini, E.; Scolaro, C.; Scopelliti, R.; Juillerat-Jeannerat, L.; Dyson, P. J. Development of organometallic ruthenium-arene anticancer drugs that resist hydrolysis. *Inorg. Chem.* **2006**, *45*, 9006−9013.
(23) Scolaro, C.; Bergamo, A.; Brescacin, L.; Delfino, R.; Cocchietto, M.; Laurenczy, G.; Geldbach, T. J.; Sava, G.; Dyson, P. J. In vitro and in vivo evaluation of ruthenium (II)-arene PTA complexes. *J. Med. Chem.* **2005**, *48*, 4161−4171.
(24) Bergamo, A.; Masi, A.; Dyson, P. J.; Sava, G. Modulation of the metastatic progression of breast cancer with an organometallic ruthenium compound. *Int. J. Oncol.* **2008**, *33*, 1281.
(25) Bergamo, A.; Gaiddon, C.; Schellens, J.; Beijnen, J.; Sava, G. Approaching tumour therapy beyond platinum drugs: status of the art and perspectives of ruthenium drug candidates. *J. Inorg. Biochem.* **2012**, *106*, 90−99.
(26) Nowak-Sliwinska, P.; van Beijnum, J. R.; Casini, A.; Nazarov, A. A.; Wagnières, G.; van den Bergh, H.; Dyson, P. J.; Griffioen, A. W. Organometallic Ruthenium(II) Arene Compounds with Antiangiogenic Activity. *J. Med. Chem.* **2011**, *54*, 3895−3902.
(27) Weiss, A.; Ding, X.; Van Beijnum, J. R.; Wong, I.; Wong, T. J.; Berndsen, R. H.; Dormond, O.; Dallinga, M.; Shen, L.; Schlingemann, R. O. Rapid optimization of drug combinations for the optimal angiostatic treatment of cancer. *Angiogenesis* **2015**, *18*, 233−244.
(28) Weiss, A.; Berndsen, R. H.; Dubois, M.; Müller, C.; Schibli, R.; Griffioen, A. W.; Dyson, P. J.; Nowak-Sliwinska, P. In vivo anti-tumor activity of the organometallic ruthenium (ii)-arene complex [Ru (η^6-*p*-cymene) Cl_2(pta)](RAPTA-C) in human ovarian and colorectal carcinomas. *Chem. Sci.* **2014**, *5*, 4742−4748.
(29) Murray, B. S.; Babak, M. V.; Hartinger, C. G.; Dyson, P. J. The development of RAPTA compounds for the treatment of tumors. *Coord. Chem. Rev.* **2016**, *306*, 86−114.
(30) Aird, R. E.; Cummings, J.; Ritchie, A. A.; Muir, M.; Morris, R. E.; Chen, H.; Sadler, P. J.; Jodrell, D. I. In vitro and in vivo activity and cross resistance profiles of novel ruthenium (II) organometallic arene complexes in human ovarian cancer. *Br. J. Cancer* **2002**, *86*, 1652−1657.
(31) Habtemariam, A.; Melchart, M.; Fernández, R.; Parsons, S.; Oswald, I. D. H.; Parkin, A.; Fabbiani, F. P. A.; Davidson, J. E.; Dawson, A.; Aird, R. E.; Jodrell, D. I.; Sadler, P. J. Structure-activity relationships for cytotoxic ruthenium(II) arene complexes containing N,N-, N,O-, and O,O-chelating ligands. *J. Med. Chem.* **2006**, *49*, 6858−6868.
(32) Betanzos-Lara, S.; Novakova, O.; Deeth, R. J.; Pizarro, A. M.; Clarkson, G. J.; Liskova, B.; Brabec, V.; Sadler, P. J.; Habtemariam, A. Bipyrimidine ruthenium(II) arene complexes: Structure, reactivity and cytotoxicity. *JBIC, J. Biol. Inorg. Chem.* **2012**, *17*, 1033−1051.
(33) Morris, R. E.; Aird, R. E.; Del Socorro Murdoch, P.; Chen, H.; Cummings, J.; Hughes, N. D.; Parsons, S.; Parkin, A.; Boyd, G.; Jodrell, D. I.; Sadler, P. J. Inhibition of cancer cell growth by ruthenium(II) arene complexes. *J. Med. Chem.* **2001**, *44*, 3616−3621.
(34) Pettinari, R.; Marchetti, F.; Condello, F.; Pettinari, C.; Lupidi, G.; Scopelliti, R.; Mukhopadhyay, S.; Riedel, T.; Dyson, P. J. Ruthenium(II)-arene RAPTA type complexes containing curcumin and bisdemethoxycurcumin display potent and selective anticancer activity. *Organometallics* **2014**, *33*, 3709−3715.
(35) Pettinari, R.; Pettinari, C.; Marchetti, F.; Skelton, B. W.; White, A. H.; Bonfili, L.; Cuccioloni, M.; Mozzicafreddo, M.; Cecarini, V.; Angeletti, M.; Nabissi, M.; Eleuteri, A. M. Arene-ruthenium(II) acylpyrazolonato complexes: Apoptosis-promoting effects on human cancer cells. *J. Med. Chem.* **2014**, *57*, 4532−4542.
(36) Marchetti, F.; Pettinari, C.; Cerquetella, A.; Cingolani, A.; Pettinari, R.; Monari, M.; Wanke, R.; Kuznetsov, M. L.; Pombeiro, A. J. L. Switching between K2 and K3 Bis(pyrazol-1-yl)acetate ligands by tuning reaction conditions: Synthesis, spectral, electrochemical, structural, and theoretical studies on arene-ru(11) derivatives of bis(azol-1-yl)acetate ligands. *Inorg. Chem.* **2009**, *48*, 6096−6108.
(37) Kandioller, W.; Balsano, E.; Meier, S. M.; Jungwirth, U.; Göschl, S.; Roller, A.; Jakupec, M. A.; Berger, W.; Keppler, B. K.; Hartinger, C. G. Organometallic anticancer complexes of lapachol: metal centre-dependent formation of reactive oxygen species and correlation with cytotoxicity. *Chem. Commun.* **2013**, *49*, 3348−3350.
(38) Kurzwernhart, A.; Kandioller, W.; Enyedy, É. A.; Novak, M.; Jakupec, M. A.; Keppler, B. K.; Hartinger, C. G. 3-Hydroxyflavones vs. 3-hydroxyquinolinones: Structure-activity relationships and stability studies on RuII(arene) anticancer complexes with biologically active ligands. *Dalton Trans.* **2013**, *42*, 6193−6202.
(39) Kurzwernhart, A.; Kandioller, W.; Bächler, S.; Bartel, C.; Martic, S.; Buczkowska, M.; Mühlgassner, G.; Jakupec, M. A.; Kraatz, H. B.; Bednarski, P. J.; Arion, V. B.; Marko, D.; Keppler, B. K.; Hartinger, C. G. Structure-Activity relationships of targeted RuII(η 6- P -Cymene) anticancer complexes with flavonol-Derived ligands. *J. Med. Chem.* **2012**, *55*, 10512−10522.
(40) Kandioller, W.; Kurzwernhart, A.; Hanif, M.; Meier, S. M.; Henke, H.; Keppler, B. K.; Hartinger, C. G. Pyrone derivatives and metals: From natural products to metal-based drugs. *J. Organomet. Chem.* **2011**, *696*, 999−1010.
(41) Lim, H.; Draelos, Z. In *Clinical Guide to Sunscreens and Photoprotection*; Informa Healthcare USA: New York, 2009.
(42) Abranches, P. A. d. S.; da Silva, E. D.; Varejão, E. V. V; Martins, C. V. B.; Ruiz, A. L. T. G.; de Resende-Stoianoff, M. A.; de Carvalho, J. E.; de Fátima, Â.; Fernandes, S. A. Antiproliferative and Antifungal Activities of 1, 3-diarylpropane-1, 3-diones Commonly used as Sunscreen Agents. *Lett. Drug Des. Discovery* **2013**, *10*, 661−665.
(43) Nitiss, J. L. Targeting DNA topoisomerase II in cancer chemotherapy. *Nat. Rev. Cancer* **2009**, *9*, 338−350.
(44) Pettinari, C.; Pettinari, R.; Fianchini, M.; Marchetti, F.; Skelton, B. W.; White, A. H. Syntheses, structures, and reactivity of new pentamethylcyclopentadienyl- rhodium(III) and -iridium(III) 4-acyl-5-pyrazolonate complexes. *Inorg. Chem.* **2005**, *44*, 7933−7942.
(45) Nakamura, Y.; Isobe, K.; Morita, H.; Yamazaki, S.; Kawaguchi, S. Several metal complexes containing acetylacetone as a neutral ligand. *Inorg. Chem.* **1972**, *11*, 1573−1578.
(46) Nakamoto, K. *Infrared and Raman Spectra of Inorganic and Coordination Compounds: Part B: Applications in Coordination, Organometallic, and Bioinorganic Chemistry*; Wiley: Hoboken, NJ, 2008; pp 1−408.
(47) Wanke, R.; Smoleński, P.; Guedes Da Silva, M. F. C.; Martins, L. M. D. R. S.; Pombeiro, A. J. L. Cu(I) complexes bearing the new sterically demanding and coordination flexible tris(3-phenyl-1-pyrazolyl)methanesulfonate ligand and the water-soluble phosphine 1,3,5-triaza-7-phosphaadamantane or related ligands. *Inorg. Chem.* **2008**, *47*, 10158−10168.
(48) Geary, W. J. The use of conductivity measurements in organic solvents for the characterisation of coordination compounds. *Coord. Chem. Rev.* **1971**, *7*, 81−122.
(49) Zeglis, B. M.; Pierre, V. C.; Barton, J. K. Metallo-intercalators and metallo-insertors. *Chem. Commun.* **2007**, 4565−4579.
(50) Markov, P.; Petkov, I. On the photosensitivity of dibenzoylmethane, benzoylacetone and ethyl benzoylacetate in solution. *Tetrahedron* **1977**, *33*, 1013−1015.
(51) Yankov, P.; Saltiel, S.; Petkov, I. Photoketonization of dibenzoylmethane in polar solvents. *Chem. Phys. Lett.* **1986**, *128*, 517−520.
(52) Veierov, D.; Bercovici, T.; Mazur, Y.; Fischer, E. Effect of additives and solvents on the fate of the primary photoproduct of 1, 3-dicarbonyl compounds. *J. Org. Chem.* **1978**, *43*, 2006−2010.
(53) Jancsó, A.; Nagy, L.; Moldrheim, E.; Sletten, E. Potentiometric and spectroscopic evidence for co-ordination of dimethyltin (IV) to phosphate groups of DNA fragments and related ligands. *J. Chem. Soc., Dalton Trans.* **1999**, 1587−1594.

DOI: 10.1021/acs.organomet.6b00694
Organometallics XXXX, XXX, XXX−XXX

(54) Pratviel, G.; Bernadou, J.; Meunier, B. DNA and RNA cleavage by metal complexes. *Adv. Inorg. Chem.* **1998**, *45*, 251−312.
(55) Ghosh, K.; Kumar, P.; Tyagi, N.; Singh, U. P.; Aggarwal, V.; Baratto, M. C. Synthesis and reactivity studies on new copper (II) complexes: DNA binding, generation of phenoxyl radical, SOD and nuclease activities. *Eur. J. Med. Chem.* **2010**, *45*, 3770−3779.
(56) Ghosh, K.; Kumar, P.; Tyagi, N. Synthesis, crystal structure and DNA interaction studies on mononuclear zinc complexes. *Inorg. Chim. Acta* **2011**, *375*, 77−83.
(57) Ju, C.-C.; Zhang, A.-G.; Yuan, C.-L.; Zhao, X.-L.; Wang, K.-Z. The interesting DNA-binding properties of three novel dinuclear Ru(II) complexes with varied lengths of flexible bridges. *J. Inorg. Biochem.* **2011**, *105*, 435−443.
(58) Kapuscinski, J. DAPI: a DNA-specific fluorescent probe. *Biotech. Histochem.* **1995**, *70*, 220−233.
(59) Biancardi, A.; Biver, T.; Secco, F.; Mennucci, B. An investigation of the photophysical properties of minor groove bound and intercalated DAPI through quantum-mechanical and spectroscopic tools. *Phys. Chem. Chem. Phys.* **2013**, *15*, 4596−4603.
(60) Nagy, E. M.; Nardon, C.; Giovagnini, L.; Marchio, L.; Trevisan, A.; Fregona, D. Promising anticancer mono- and dinuclear ruthenium-(iii) dithiocarbamato complexes: systematic solution studies. *Dalton Trans.* **2011**, *40*, 11885−11895.
(61) Anderson, C. M.; Taylor, I. R.; Tibbetts, M. F.; Philpott, J.; Hu, Y.; Tanski, J. M. Hetero-multinuclear Ruthenium(III)/Platinum(II) Complexes That Potentially Exhibit Both Antimetastatic and Antineoplastic Properties. *Inorg. Chem.* **2012**, *51*, 12917−12924.
(62) Vuradi, R. K.; Putta, V. R.; Nancherla, D.; Sirasani, S. Luminescent Behavior of Ru(II) Polypyridyl Morpholine Complexes, Synthesis, Characterization, DNA, Protein Binding, Sensor Effect of Ions/Solvents and Docking Studies. *J. Fluoresc.* **2016**, *26*, 689−701.
(63) Mukhopadhyay, S.; Gupta, R. K.; Paitandi, R. P.; Rana, N. K.; Sharma, G.; Koch, B.; Rana, L. K.; Hundal, M. S.; Pandey, D. S. Synthesis, Structure, DNA/Protein Binding, and Anticancer Activity of Some Half-Sandwich Cyclometalated Rh(III) and Ir(III) Complexes. *Organometallics* **2015**, *34*, 4491−4506.
(64) Messori, L.; Vilchez, F. G.; Vilaplana, R.; Piccioli, F. Binding of Antitumor Ruthenium (Ill) Complexes to Plasma Proteins. *Met.-Based Drugs* **2000**, *7*, 335.
(65) Dömötör, O.; Hartinger, C. G.; Bytzek, A. K.; Kiss, T.; Keppler, B. K.; Enyedy, E. A. Characterization of the binding sites of the anticancer ruthenium(III) complexes KP1019 and KP1339 on human serum albumin via competition studies. *JBIC, J. Biol. Inorg. Chem.* **2013**, *18*, 9−17.
(66) Casini, A.; Gabbiani, C.; Sorrentino, F.; Rigobello, M. P.; Bindoli, A.; Geldbach, T. J.; Marrone, A.; Re, N.; Hartinger, C. G.; Dyson, P. J.; Messori, L. Emerging protein targets for anticancer metallodrugs: Inhibition of thioredoxin reductase and cathepsin B by antitumor ruthenium(II)-arene compounds. *J. Med. Chem.* **2008**, *51*, 6773−6781.
(67) Babak, M. V.; Meier, S. M.; Huber, K. V. M; Reynisson, J.; Legin, A. A.; Jakupec, M. A.; Roller, A.; Stukalov, A.; Gridling, M.; Bennett, K. L.; Colinge, J.; Berger, W.; Dyson, P. J.; Superti-Furga, G.; Keppler, B. K.; Hartinger, C. G. Target profiling of an antimetastatic RAPTA agent by chemical proteomics: Relevance to the mode of action. *Chem. Sci.* **2015**, *6*, 2449−2456.
(68) Xu, L.; Zhong, N.-J.; Xie, Y.-Y.; Huang, H.-L.; Jiang, G.-B.; Liu, Y.-J. Synthesis, characterization, in vitro cytotoxicity, and apoptosis-inducing properties of ruthenium (II) complexes. *PLoS One* **2014**, *9*, e96082.
(69) Smoleński, P.; Kirillov, A. M.; Da Silva, M. F. C. G.; Pombeiro, A. J. L. 1-Methyl-1-azonia-3,5-diaza-7-phosphatricyclo-[3.3.1.13,7]-decane tetrafluoroborate. *Acta Crystallogr., Sect. E: Struct. Rep. Online* **2008**, *64*, o556.
(70) Duisenberg, A. J. M.; Kroon-Batenburg, L. M. J.; Schreurs, A. M. M. An intensity evaluation method: EVAL-14. *J. Appl. Crystallogr.* **2003**, *36*, 220−229.
(71) Blessing, R. H. An empirical correction for absorption anisotropy. *Acta Crystallogr., Sect. A: Found. Crystallogr.* **1995**, *51*, 51.
(72) Sheldrick, G. M. A short history of SHELX. *Acta Crystallogr., Sect. A: Found. Crystallogr.* **2008**, *64*, 112−122.
(73) Marmur, J. A procedure for the isolation of deoxyribonucleic acid from micro-organisms. *J. Mol. Biol.* **1961**, *3*, 208−218.
(74) Bi, S.; Yan, L.; Pang, B.; Wang, Y. Investigation of three flavonoids binding to bovine serum albumin using molecular fluorescence technique. *J. Lumin.* **2012**, *132*, 132−140.
(75) Min, J.; Meng-Xia, X.; Dong, Z.; Yuan, L.; Xiao-Yu, L.; Xing, C. Spectroscopic studies on the interaction of cinnamic acid and its hydroxyl derivatives with human serum albumin. *J. Mol. Struct.* **2004**, *692*, 71−80.
(76) Gratton, E.; Silva, N.; Mei, G.; Rosato, N.; Savini, I.; Finazzi-Agro, A. Fluorescence lifetime distribution of folded and unfolded proteins. *Int. J. Quantum Chem.* **1992**, *42*, 1479−1489.
(77) Zaitsev, E. N.; Kowalczykowski, S. C. Binding of double-stranded DNA by Escherichia coli RecA protein monitored by a fluorescent dye displacement assay. *Nucleic Acids Res.* **1998**, *26*, 650−654.

DOI: 10.1021/acs.organomet.6b00694
Organometallics XXXX, XXX, XXX−XXX